Available online at www.sciencedirect.com

ScienceDirect

Ceramics International 40 (2014) 3131–3138

CERAMICS INTERNATIONAL

www.elsevier.com/locate/ceramint

High performance $BaCe_{0.8}Y_{0.2}O_{3-a}$ (BCY) hollow fibre membranes for hydrogen permeation

Xihan Tan[a], Xiaoyao Tan[a,b], Naitao Yang[a], Bo Meng[a,*], Kun Zhang[c], Shaomin Liu[c,**]

[a]School of Chemical Engineering, Shandong University of Technology, Zibo 255049, China
[b]Department of Chemical Engineering, Tianjin Polytechnic University, Tianjin 300387, China
[c]Department of Chemical Engineering, Curtin University, Perth, WA 6845, Australia

Received 10 September 2013; received in revised form 28 September 2013; accepted 28 September 2013
Available online 8 October 2013

Abstract

In this work, $BaCe_{0.8}Y_{0.2}O_{3-\alpha}$ (BCY) perovskite hollow fibre membranes were fabricated by a phase inversion and sintering method. BCY powder was prepared by the sol–gel technique using ethylenediaminetetraacetic acid (EDTA) and citric acid as the complexing agents. Gel calcination was carried out at high temperature to form the desired crystal structure. The qualified BCY hollow fibre membranes could not be achieved even the sintering was carried out at temperatures up to 1550°C due to the poor densification behavior of the BCY material. The addition of sintering aid (1 wt% Co_2O_3) inside BCY powder as the membrane starting material significantly improved the densification process, leading to the formation of gas-tight BCY hollow fibres. The optimum sintering temperature of BCY hollow fibre membrane was 1400 °C to achieve the best mechanical strength. H_2 permeation through the BCY hollow fibre membranes was carried out between 700 and 1050 °C using 25% H_2–He mixture as feed gas and N_2 as sweep gas, respectively. For comparison purpose, the disk-shaped BCY membrane with a thickness of 1 mm was also prepared. The measured H_2 permeation flux through the BCY hollow fibres reached up to 0.38 mL cm^{-2} min^{-1} at 1050 °C strikingly contrasting to the low values of less than 0.01 mL cm^{-2} min^{-1} from the disk-shaped membrane. After the permeation test, the microstructure of BCY hollow fibre membrane was still maintained well without signals of membrane disintegration or peeling off.

Keywords: A. Extrusion; A. Sintering; D. Perovskites; E. Membranes; Hydrogen permeation

1. Introduction

Since the pioneering work by Iwahara et al. [1,2] dense protonic conducting ceramic membranes based on $SrCeO_3$, $BaCeO_3$, $SrZrO_3$ and $BaZrO_3$ perovskite oxides in a general formula of ABO_3, have attracted considerable attention in the research fields of high temperature electrochemical devices like fuel cells, sensors, galvanic hydrogen pumps or hydrogen selective membrane reactors to replace the expensive Pd membranes [3–11]. An undoped perovskite oxide such as pure $BaCeO_3$ would not possess the desired proton conduction. The appearance of proton conducting property of these perovskites is closely associated with their oxygen vacancies which can be created by the charge compensation when these perovskite oxides are doped with aliovalent cations. For instance, the substitution of 0.2 mole Ce^{4+} by Y^{3+} in $BaCeO_3$ provides 0.1 mole oxygen vacancies in the resultant perovskite with the apparent formula of $BaCe_{0.8}Y_{0.2}O_{2.9}$. These proton conducting oxides share one common feature. They do not have the host constituent to liberate conducting protons, but have to take the protons from water vapour or hydrogen molecules in ambient via the surface reactions between the defects and gas [2–4]. The formed protons can migrate by hopping from one O^{2-} to another in the nearest neighbouring position heading to the other membrane side [11,12]. In a strict sense, all these doped perovskite oxides are mixed conductors displaying not only the proton conductivity but also other kinds like oxygen ionic or electronic conductivity. The dominated type of conductivity normally determines their application categories. For example,

*Corresponding author. Tel.: +86 5332786292.
**Corresponding author. Tel.: +61 8 92669056.
E-mail addresses: mb1963@126.com (B. Meng), shaomin.liu@curtin.edu.au (S. Liu).

0272-8842/$ - see front matter © 2013 Elsevier Ltd and Techna Group S.r.l. All rights reserved.
http://dx.doi.org/10.1016/j.ceramint.2013.09.132

when the proton conductivity is far larger than oxygen ionic or electronic conductivities, these doped $SrCeO_3$ or $BaCeO_3$ based perovskite ceramics can be used as proton conductor. When the conductivities are contributed significantly by both proton (or oxygen ionic) and electronic conductivities, these perovskite oxides can be applied as the mixed conducting membranes for hydrogen (or oxygen) separation without the necessity of external electric loadings and power source, which greatly simplifies the membrane design/fabrication and thus spurs a lot of interest for gas separation for clean energy application purposes [2,4,6,8,10,13]. The gas permeation flux value of these mixed conducting membranes is not only dependent on the materials and membrane morphology but also varying with the operating conditions like downstream gas atmosphere [6]. To apply these proton conductors as the non-galvanic mixed conducting membranes, their electronic conductivity must be improved. To this end, much effort has been done on optimizing the perovskite compositions of $SrCe_{(1-x)}M_xO_{(3-0.5x)}$ or $BaCe_{(1-x)}M_xO_{(3-0.5x)}$ using a better dopant M^3 such as Y, Yb, Sm, Eu, Tm, Tb, Ti, V, Cr, Mn, Co, Ni, Cu, Al, Ga and In at different concentrations (x: 5−20%) [14–20] or to disperse a metal phase (Pd, Ag, Cu, Ni, Nb, Ta, Zr, etc. in 10–50 vol%) inside the perovskite matrix to form the cermet membranes [21,22]. Electronic conductivity is also affected by the downstream gas atmosphere; thus another way is to change the operating conditions to be more favourable for electronic conduction. This can be realized by introducing some reducing gases like CO or hydrogen inside the sweep gas. One good example is the H_2 permeation through the Tb doped $SrCeO_3$ membrane exposed to H_2/He gradient or H_2/(He+CO) gradient [6]. Swept by the inert gas (He) or air, no any H_2 permeation was detected. However, with the introduction of CO up to 100 ppm inside the sweep gas, H_2 flux was significantly improved. Once H_2 permeation was triggered by the presence of CO, it would be continued even switching off the CO flow since the permeated H_2 could play the same role of the CO to further decrease the O_2 partial pressure inside the sweep gas by reducing reactions. Certainly, temperature is another driving force as these oxide membranes need to be operated under high temperatures.

Form the point view of the membrane synthesis, the membrane should be prepared as thin as possible to decrease the transport resistance, but it must be sufficiently robust to withstand the gas pressures and the thermal expansion stress as these ceramic membranes are usually sealed at room temperature but used at high temperature. Disk-shaped membranes with large thickness of 1 mm were employed in most of these studies of the doped $SrCeO_3$ or $BaCeO_3$ based proton conductors as the synthesis is relative easier compared to these supported thin membranes. The hydrogen flux through these membranes with large thickness swept by inert gas is in the order of 10^{-9} mol cm^{-2} s^{-1} (or 10^{-3} mL cm^{-2} min^{-1}) or less [6,11,15–18]. Apparently, membrane thickness reduction will also lead to the improved membrane performance. Recently, in the field of mixed conducting ceramic membranes for oxygen separation, hollow fibre geometry has been widely adopted because of its larger membrane area per unit packing volume, easier sealing for the high temperature test and in particular a very thin self-supported separating layer in the occasion that the hollow fibre is prepared by the phase-inversion method [23–26]. Despite of these advantages, the application of hollow fibre geometry for proton conducting membranes is rarely attempted [27,28]. One possible reason lies in the difficulty to prepare the qualified (or gastight) membranes as these proton-conducting ceramics normally have very high melting points exemplified by $BaCeO_3$ and $SrCeO_3$ with their respective melting points of 2016 and 2266 K [29]. To achieve the desired densification, these ceramics need to be sintered at a super-high temperature. Addition of small amount of sintering aids like ZnO, Co_2O_3, CuO etc. may help to lower the sintering temperature [30].

The objective of this research is to improve the H_2 permeation fluxes through these doped $SrCeO_3$ or $BaCeO_3$ based proton conducting membranes by the hollow fibre membrane technology. We examined the feasibility of using sintering aid to facilitate the preparation of proton conducting perovskite hollow fibre membranes and investigated the hydrogen permeation behavior. $BaCe_{0.8}Y_{0.2}O_{3-\ddot{a}}$ (BCY) not only exhibits high proton conductivity but also displays a certain level of electronic conductivity, therefore, was chosen as the hollow fibre material in the present study. The used sintering aid was Co_2O_3 in 1 wt % inside the hollow fibre material.

2. Experimental

2.1. Fabrication of the BCY perovskite powder, BCY hollow fibre and disk-shaped membranes

The $BaCe_{0.8}Y_{0.2}O_{3-\ddot{a}}$ (BCY) perovskite powder was synthesized by a sol–gel method using ethylenediaminetetraacetic acid (EDTA) and citric acid (CA) as complexing agents simultaneously. $Ba(NO_3)_2$, $Ce(NO_3)_3 \cdot 6H_2O$, $Y(NO_3)_3 \cdot 6H_2O$, all in analytical grades, were used as the raw materials for metal ion sources. The mole ratio of total metal ions to EDTA and citric acid in the sol was 1:1.5:1.2. The powder precursor obtained by the gel combustion was calcined at 1000 °C for 5 h under static air to obtain the perovskite phase. The detailed synthesis process was described elsewhere [31]. For spinning hollow fibre membrane precursors, the calcined powder was further ball-milled in the presence of alcohol for at least 10 h followed by sieving through a sifter of 200-mesh to exclude larger agglomerates.

The BCY hollow fibre membranes were prepared by the phase inversion and sintering technique [25,27]. The starting suspension was composed of 66.67 wt% BCY powder, 6.67 wt% polyethersulfone (PESf, Radel A-300, from Ameco Performance, USA) as the polymer binder and 26.67 wt% N-methyl-2-pyrrolidone (NMP, AR Grade, > 99.8%, Kermel Chem. Inc., Tianjin, China) as the solvent. A spinneret with the orifice diameter/inner diameter of 3.0/1.2 mm was used for spinning hollow fibre precursors. Tap water and deionised water were used as the external and the internal coagulants, respectively. Sintering was

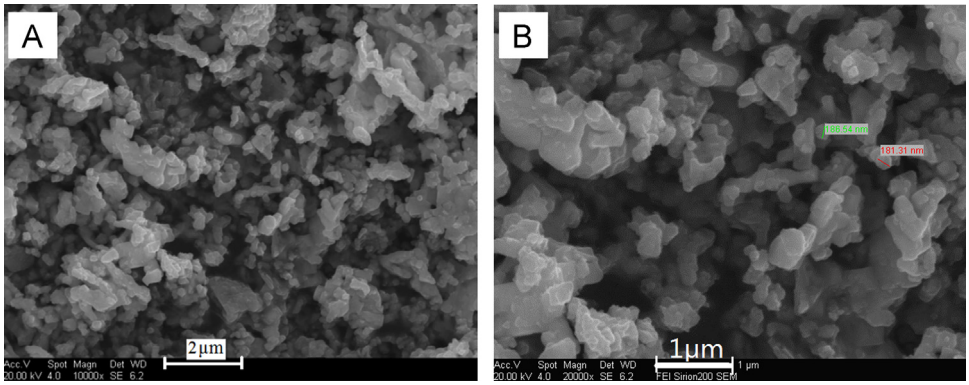

Fig. 1. SEM images of $BaCe_{0.8}Y_{0.2}O_{3-\delta}$ powder prepared at 1000 °C.

performed at the elevated temperatures ranging from 1200 to 1550 °C for 5 h under ambient non-flowing air atmosphere. The heating and cooling rate applied during the whole sintering process was 2–4 °C min^{-1}. In the meantime, the BCY disk membrane (diameter of 25 mm and thickness of 1 mm) was prepared by statically pressing the pure BCY powder under a pressure of 10 MPa followed by sintering at 1550 °C for 5 h.

2.2. Characterization

Microstructures of the BCY powder and hollow fibres were observed by scanning electron microscopy (SEM) (FEI Sirion 200, Netherlands). Gold sputter coating was performed on the samples under vacuum before the measurements. The crystal structures of the samples were measured by an X-ray diffractometer (XRD: D8 Advance, Germany) using Cu-Ka radiation (λ=0.15404 nm). A continuous scan mode was used to collect 2θ data from 20° to 80° with a 0.02 sampling pitch and a 2° min^{-1} scan rate. X-ray tube voltage and current were set at 40 kV and 30 mA, respectively. The gas-tightness of the hollow fibres was examined by the gas permeation measurement using N_2 as the test gas at room temperature [32]. The mechanical strength of the hollow fibres was measured on a three-point bending instrument (Instron Model 5544) with a crosshead speed of 0.5 mm min^{-1}.

2.3. Hydrogen permeation measurement

Only these membranes displaying gas tight at room temperature were chosen for hydrogen permeation. The hydrogen flux through the hollow fibre membranes with length of 25 cm was tested using a home-made high-temperature permeation cell with details previously described elsewhere [33]. The effective uniform heating length of the tube furnace is 5 cm. The H_2–He mixture with the molar ratio of 1:1 was fed to the shell side while nitrogen as the sweep gas was introduced in the fibre lumen to collect the permeated hydrogen for concentration detection. The flow rates of the H_2–He feed and the N_2 sweep gas were controlled by mass flow controllers (D08-8B/ZM, Shanxi Chuangwei Instrument Co. Ltd, China) which were calibrated with a soap bubble flow metre. The effluent flow rate of the permeate stream was also measured by the soap bubble flow metre. The composition of the permeated gas was analyzed with a gas chromatograph (Agilent 6890) fitted with a carbon molecular sieve column (4 m in length) using highly pure argon as the carrier gas. The hydrogen permeation flux was calculated according to the method that can be found elsewhere [28].

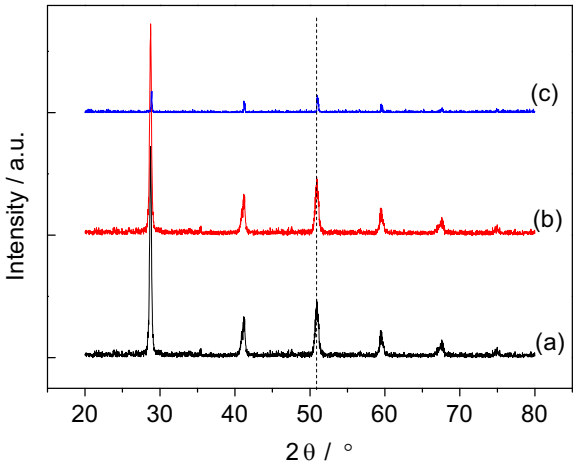

Fig. 2. XRD patterns of the BCY powder (a), BCY hollow fibre (b) and BCY+Co_2O_3 hollow fibre (c) [BCY powder were prepared at 1000 °C; BCY and BCY+Co_2O_3 (1%) hollow fibres were sintered at 1400 °C].

3. Results and discussion

The BCY powder with desired crystalline structure was prepared by the sol–gel method using the combined complexing agents of ethylenediaminetetraacetic acid (EDTA) and citric acid (CA) with subsequent calcination of the powder precursor at high temperature of 1000 °C. The SEM image of Fig. 1A depicts the porous morphology of the BCY particle agglomerates. A closer inspection on the SEM image (Fig. 1B) at higher magnification illustrates the grain size of the BCY particle is around 180 nm. Fig. 2a displays the XRD pattern of the prepared BCY powder with the characteristic peaks at the respective 2θ angles of 28.699° (211), 40.934° (220), 50.801°

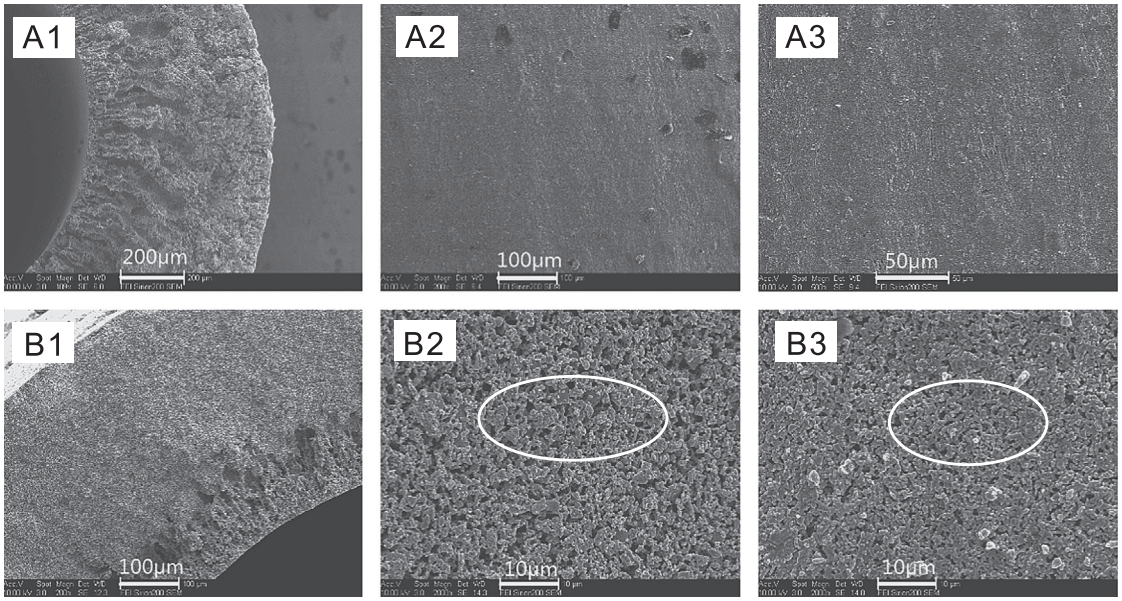

Fig. 3. SEM images of BCY hollow fibre precursor (A1–A3) and the BCY hollow fibre membrane sintered at 1550 °C without sintering aid (B1–B3) [1: cross-section; 2: outside surface; 3: inside surface.

(213), 59.428° (422), 67.165° (233) and 74.759° (404) which are closely matching the reported perovskite structure [28,34]. The grain growth was caused by grain contact and coalescence during the high temperature treatment. However, the presence of large particle agglomerate is not favourable to prepare a pinhole-free BCY hollow fibre. Prior to the mixing with organic binder, such agglomerates should be broken into smaller particles by ball-milling treatment. Fig. 2b shows the XRD patterns of the BCY hollow fibres heated at 1400 °C.

Fig. 3 shows the SEM images of the prepared the hollow fibre precursor and the sintered BCY hollow fibre without the sintering aid. The SEM images were taken from the cross sectional and surface views. The porous structure with different porosity (Fig. 3A1) in the cross sectional area is a typical characteristic derived from the phase inversion technique which is widely used to prepare polymeric hollow fibre membranes. Due to the higher binding capability of the polymer (PESF), the dispersed BCY particles were strongly bound together to maintain the hollow fibre shape and routine handling. The sintered BCY hollow fibre to be used for the hydrogen permeation must be sufficiently dense to block the direct passage of any molecular gases. For this purpose, the BCY hollow fibres were sintered at temperatures higher than 1300 °C. However, all these BCY membranes displayed severe gas leakage at room temperature and could not be used for H_2 permeation test. As can be seen from Fig. 3B, even sintered at 1550 °C, the morphology of the BCY hollow fibre surfaces was still in highly porous structure with pore size as large as 5 μ (marked with white rings) in the two surfaces. To have the BCY with a desired densification, the sintering temperature must be further improved above 1550 °C. However, this oversintering may lead to the loss of some easily evaporated elements like barium and introduce an uncertainty to the elemental composition. Thus the addition of sintering aid is very necessary to better sinter these ceramics with high melting points. Fig. 4 shows the sintered BCY membranes with the addition of 1 wt% of Co_2O_3. As can be seen, the sintering was strikingly improved. Even at much lower temperatures like 1350 °C, the BCY membrane already displayed the required densification and gas-tightness for H_2 permeation evidenced by the removal of closed or thoroughly connected pores by grain growth or volumetric shrinkage. SEM images of surface morphology in Fig. 4B2–D2 and B3–D3 clearly show the average grain size growth to 2, 3 and 5 μ by sintering at 1350, 1400 and 1450 °C, respectively. The gas leaking test at room temperature verified their gas-tightness. Compared to the BCY preparation without sintering aid, the required sintering temperature was lowered at least by 200 °C to reach the desired densification. The improved sintering with Co_2O_3 is possibly through a mechanism involving liquid-assisted sintering or the formation of A-site cation-deficient BCY as cobalt is easily incorporated into the B-site of the perovskite ABO_3 structure. Given that a higher content of sintering aid may cause the change of stoichiometric composition of BCY and negatively affect the ion transportation, the addition of Co_2O_3 was only limited to 1 wt%. As predicted, the XRD pattern of BCY-Co fibre (Fig. 2c) does not display any difference from pure BCY fibre (Fig. 2b) or BCY powder (Fig. 2a). Improved densification was also accompanied by the increase of mechanical strength with data displaying in Fig. 5. The maximum bending strength around 180 MPa of the BCY-Co membrane was obtained at an optimum temperature of 1400 °C, after which the strength started to drop down, for instance, with a lower value of 158 MPa at 1450 °C. The reason for such detrimental effect of the sintering temperatures higher than 1400 °C on the mechanical strength is possibly due to the phase separation of

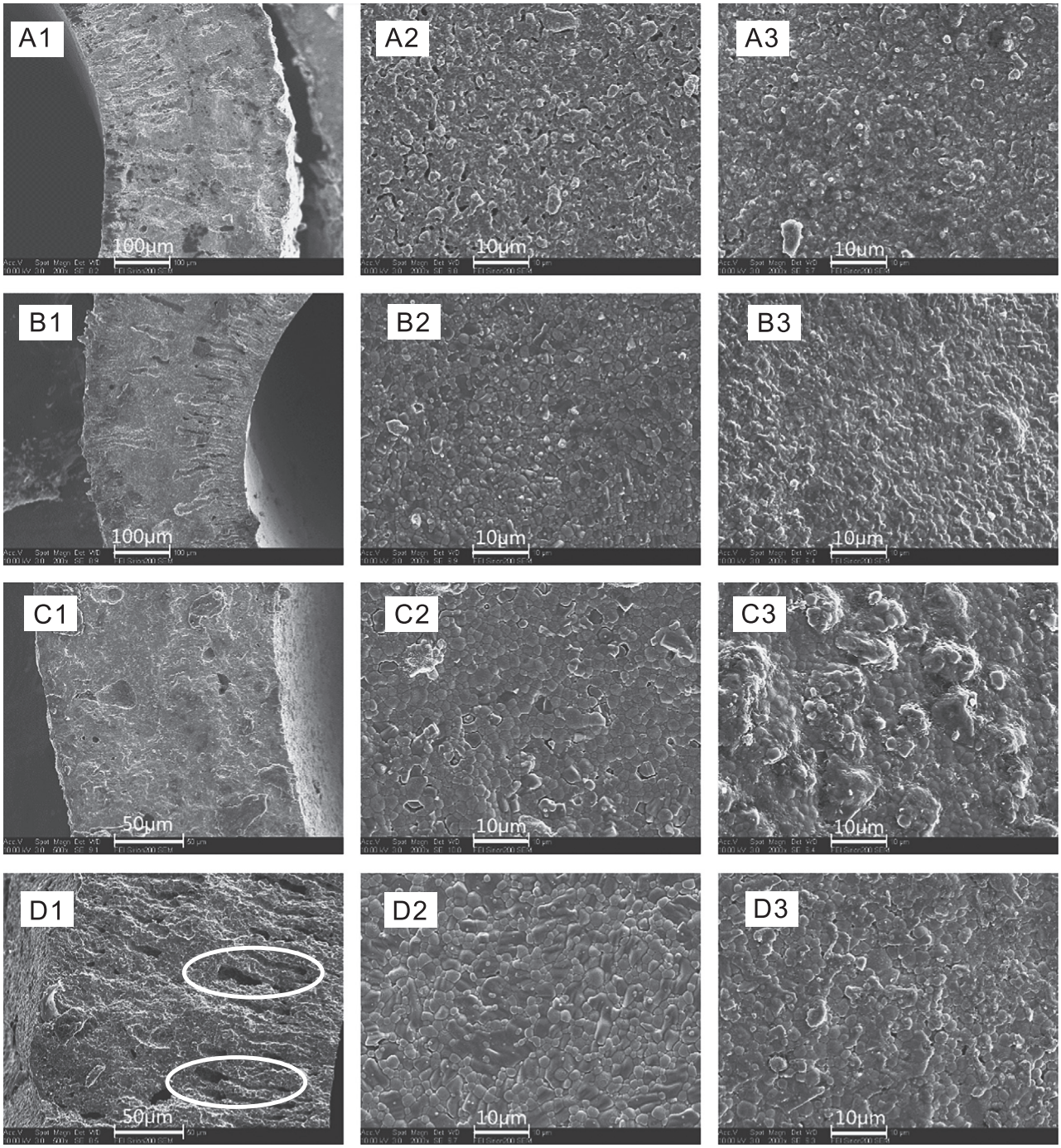

Fig. 4. SEM images of the sintered BCY hollow fibre membranes with sintering aid of 1 wt% Co_2O_3 [A: 1300 °C; B: 1350 °C; C: 1400 °C; D: 1450 °C; 1: cross-section; 2: outside surface; 3: inside surface].

$BaCeO_3$, which was repeatedly observed on other cerium oxide based perovskites [27,28]. At higher temperatures near its melting point (1480 °C), $BaCeO_3$ would be separated into solid phase CeO_2 and a liquid phase rich of BaO [35]. The easy evaporation of liquid BaO not only altered the initially designed material composition but also damaged the mechanical strength. Looking back at the SEM image of the cross sectional area in Fig. 4D1, the overall integral structure of the hollow fibre was impaired by such phase separating behavior evidenced by the presence of large porous channels marked by white shapes. However, such detrimental effects brought by higher sintering temperature on the physical properties of the sintered perovskites were only observed on hollow fibres, but not on flat membranes with larger thickness. This indicates that the preparation of qualified densified perovskite hollow fibres is more challenging and thus the sintering condition should be more carefully controlled than that of disk-shaped membranes.

Hydrogen permeation tests were performed on these gas tight BCY hollow fibre membranes sintered at 1400 °C because these hollow fibres provide the best mechanical strength for routine

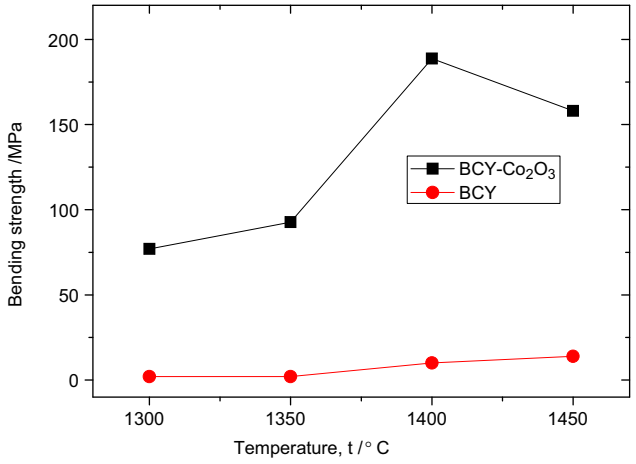

Fig. 5. Mechanical strength of the BCY hollow fibres with and without sintering aid sintered at different temperatures.

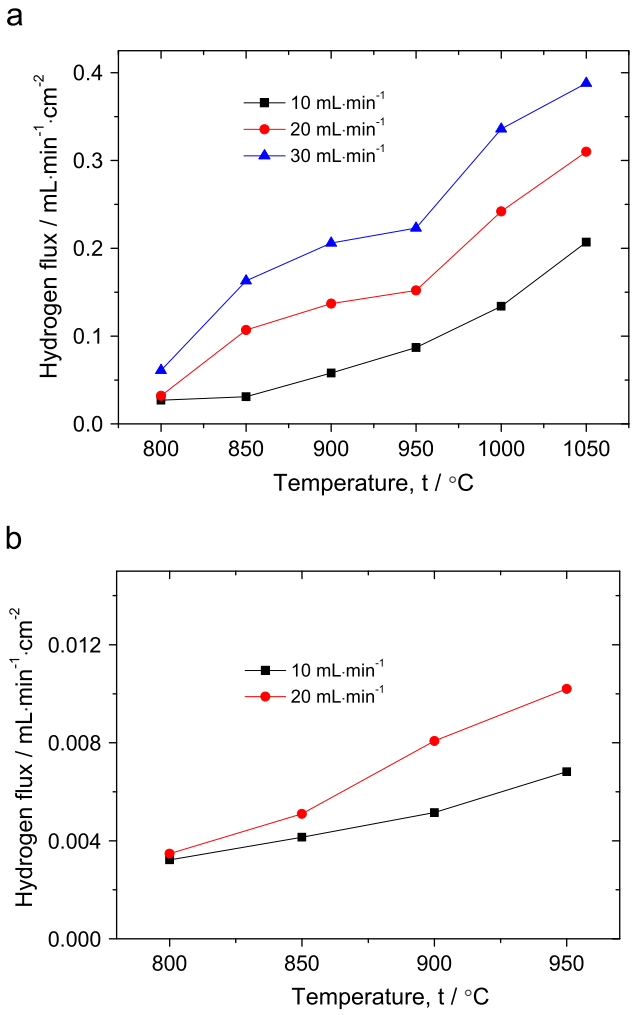

Fig. 6. Hydrogen permeation fluxes through the 1400 °C-sintered BCY hollow fibre membrane (a) and 1-mm-thick disk shaped BCY membrane (b) with different N_2 sweep flow rates [50% H_2–He feed flow rate].

assembling the membrane module without breaking. Fig. 6 displays the experimental results of H_2 fluxes versus operating temperatures where the feed flow rate of the H_2–He mixture (1:4) was fixed at 100 mL min^{-1} and the N_2 sweeping rate was varied from 10 to 30 mL min^{-1}. As expected by a general rule, H_2 flux increased with temperature increment since both the surface reactions and the bulk ionic diffusion needed to be thermally activated and were enhanced by a higher temperature environment. For example, the hydrogen flux rose from 0.06 to 0.21 mL cm^{-2} min^{-1} as the temperature was improved from 800 to 900 °C at the nitrogen sweeping rate of 30 mL min^{-1}. Another driver for the H_2 permeation is the H_2 partial pressure gradient; thus lowering the H_2 partial pressure at the permeate side by a higher sweeping flow rate would also promote the H_2 permeation. For instance, increasing the nitrogen flow rate from 10 to 30 mL min^{-1} boosted the H_2 flux from 0.13 to 0.34 mL cm^{-2} min^{-1} at 1000 °C. These trends were normally observed in the operation of mixed conducting ceramic membranes for gas production or separations [23–26]. During our investigation, the maximum H_2 flux of 0.38 mL cm^{-2} min^{-1} was achieved at 1050 °C with a sweep gas flow rate of 30 mL min^{-1}. For comparison purpose, a disk-shaped BCY membrane with a thickness of 1 mm was also prepared at 1550 °C for 5 h and tested for H_2 permeation. As showing in Fig. 6b, the general trend of H_2 flux values through the disk membrane versus temperatures and sweep gas flow rates is similar to that of hollow fibres. However, the H_2 flux values of the disk membrane are very low compared to the hollow fibres. Operated from 800 to 950 °C, the BCY disk membrane displayed H_2 fluxes in the order of 0.001 mL cm^{-2} min^{-1}. Such low fluxes were also observed from other doped proton conductors like Yb, Eu, or Tm doped $SrCeO_3$ membranes with a thickness from 1–1.5 mm [6,11,15–18]. Compared to these plate membranes, the flux values of BCY hollow fibre have been improved by a factor up to two orders of magnitude at relative similar conditions. Such a drastic increase in hydrogen permeation flux can be attributed to the reduced membrane thickness with examples shown in Fig. 4B1 or 4C1 of less than 200 μ. In addition to the high membrane surface area per unit volume, another advantage of using BCY hollow fibre is its relative easier membrane sealing. The two sealing ends can be kept away from the high temperature zone and thus the permeation test of BCY hollow fibre could be as high as 1050 °C. By contrast, the entire area of the plate membrane and the sealing was exposed to the high temperature atmosphere and thus could only be tested maximally at 950 °C, beyond which the sealing materials cannot tolerate. Fig. 7 displayed the SEM images of the BCY hollow fibre after the H_2 permeation test for 12 h at high temperatures. Inspected from the cross sectional and surface views, the general integration of BCY membrane structure was still well maintained without any signs of peeling off or disintegration.

4. Conclusions

Gas-tight $BaCe_{0.8}Y_{0.2}O_{3-\alpha}$ (BCY) perovskite hollow fibre membranes were fabricated by the combined phase inversion and sintering technique. As the starting membrane material, the BCY powder precursor was synthesized by the sol–gel method and subsequently calcined at 1000 °C to form the desired

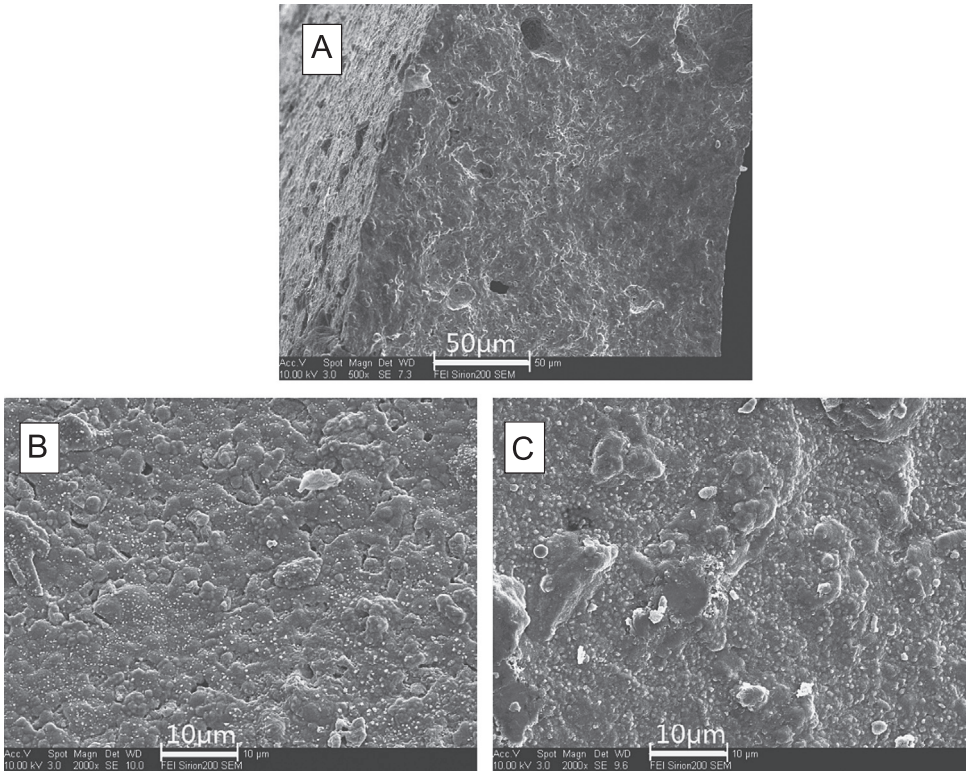

Fig. 7. SEM images of the tested BCY hollow fibre membranes [A: cross-section; B: outside surface; C: inside surface

perovskite structure. The sintering aid of Co_2O_3 has a profound influence on the gas-tightness of the resultant BCY hollow fibres. Without the sintering aid, the required densification to make the BCY hollow fibre gas-tight could not be achieved even sintering was carried out at high temperatures as high as 1550 °C. With the addition of only 1 wt% Co_2O_3 inside the BCY, densification was improved significantly and gas-tight BCY hollow fibre membrane was successfully obtained at sintering temperatures much lower than 1550 °C. The optimum sintering temperature is 1400 °C, offering the BCY fibres the best mechanical strength. H_2 permeation was tested at high temperatures using an inert sweep gas mode. The maximum H_2 flux through the BCY hollow fibre membrane under investigated conditions from 800 to 1050 °C with sweep gas flow rate varying from 10 to 30 mL min^{-1} was 0.38 mL cm^{-2} min^{-1}. The hollow fibre geometry gave the flux values at least 15 times that of BCY disk-shaped membrane. Compared to other doped $SrCeO_3$ mixed proton and electronic conducting membranes reported in the literature, the prepared BCY hollow fibre membrane also improved the H_2 flux value by a factor up to two orders of magnitude.

Acknowledgements

The authors gratefully acknowledge research funding from the Natural Science Foundation of China (No. 21176146 and No. 20976098) and the financial support provided by the Australian Research Council through the Future Fellow Program (FT12100178).

References

[1] H. Iwahara, Technological challenges in the application of proton conducting ceramics, Solid State Ionics 77 (1995) 289–298.
[2] S. Hamakawa, T. Hibino, H. Iwahara, Electrochemical hydrogen in a proton–hole mixed conductor and its application to a membrane reactor, Journal of The Electrochemical Society 141 (1994) 1720–1725.
[3] H. Iwahara, Hydrogen pumps using proton-conducting ceramics and their applications, Solid State Ionics 125 (1999) 271–278.
[4] T. Norby, Y. Larring, Mixed hydrogen ion–electronic conductors for hydrogen permeable membranes, Solid State Ionics 136–137 (2000) 139–148.
[5] G. Marnellos, S. Zisekas, M. Stoukides, Synthesis of ammonia at atmospheric pressure with the use of solid state proton conductors, Journal of Catalysis 193 (2000) 80–87.
[6] X. Wei, J. Kniep, Y.S. Lin, Hydrogen permeation through terbium doped strontium cerate membranes enabled by presence of reducing gas in the downstream, Journal of Membrane Science 345 (2009) 201–206.
[7] S. Liu, X. Tan, K. Li, R. Hughes, Methane coupling using membrane reactors, Catalysis Reviews 43 (2001) 147–198.
[8] M. Cai, S. Liu, K. Efimov, J. Caro, A. Feldhoff, H. Wang, Preparation and hydrogen permeation of $BaCe_{0.95}Nd_{0.05}O_{3-\delta}$ membranes, Journal of Membrane Science 343 (2009) 90–96.
[9] H. Iwahara, Y. Asakura, K. Katahira, M. Tanaka, Prospect of hydrogen technology using proton-conducting ceramics, Solid State Ionics 168 (2004) 299–310.
[10] S.J. Song, J.H. Moon, H.W. Ryu, T.H. Lee, S.E. Dorris, U. Balachandran, Non-galvanic hydrogen production by water splitting using cermet membranes, Journal of Ceramics Processing Research 9 (2008) 123–125.

[11] X. Qi, Y.S. Lin, Electrical conducting properties of proton-conducting terbiumdoped strontium cerate membrane, Solid State Ionics 120 (1999) 85–93.
[12] S.D. Flint, R.C.T. Slade, Variations in ionic conductivity of calcium-doped barium cerate ceramic electyrolytes in different atmopsheres, Solid State Ionics 97 (1997) 457–464.
[13] G.T. Li, G.X. Xiong, S.S. Sheng, W.S. Yang, Hydrogen permeation properties of perovskite-type $BaCe_{0.9}Mn_{0.1}O_{3-\delta}$ dense ceramic membrane, Chinese Chemical Letters 12 (2001) 937–940.
[14] X. Qi, Y.S. Lin, Electrical conducting properties of proton-conducting terbiumdoped strontium cerate membrane, Solid State Ionics 120 (1999) 85–93.
[15] S. Hamakawa, L. Li, A. Li, E. Iglesia, Synthesis and hydrogen permeation properties of membranes based on dense $SrCe_{0.95}Yb_{0.05}O_3-a$ thin films, Solid State Ionics 148 (2002) 71–81.
[16] S.J. Song, E.D. Wachsman, J. Rhodes, S.E. Dorris, U. Balachandran, Hydrogen permeability of $SrCe_{1-x}M_xO_{3-1}$ ($x=0.05$, M=Eu, Sm), Solid State Ionics 167 (2004) 99–105.
[17] D. Dionysiou, X. Qi, Y.S. Lin, G. Meng, D. Peng, Preparation and characterization of proton conducting terbium doped strontium cerate membranes, Journal of Membrane Science 154 (1999) 143–153.
[18] X. Qi, Y.S. Lin, Electrical conduction and hydrogen permeation through mixedproton–electron conducting strontium cerate, Solid State Ionics 130 (2000) 149–156.
[19] J. Guan, S.E. Dorris, U. Balachandran, M. Liu, Transport properties of $SrCe_{0.95}Y_{0.05}O_{3-a}$ and its application for hydrogen separation, Solid State Ionics 110 (1998) 303–310.
[20] X. Wei, Y.S. Lin, Protonic and electronic conductivities of terbium doped strontium cerates, Solid State Ionics 178 (2008) 1804–1810.
[21] U. Balachandran, T.H. Lee, L. Chen, S.J. Song, J.J. Picciolo, S.E. Dorris, Hydrogen separation by dense cermet membranes, Fuel 85 (2006) 150–155.
[22] S.J. Song, J.H. Moon, T.H. Lee, S.E. Dorris, U. Balachandran, Thickness dependence of hydrogen permeability for Ni–$BaCe_{0.8}Y_{0.2}O_3-a$, Solid State Ionics 179 (2008) 1854–1857.
[23] X. Tan, Y. Liu, K. Li, Preparation of LSCF ceramic hollow fibre membranes for oxygen production by a phase-inversion/sintering technique, Industrial & Engineering Chemistry Research 44 (2005) 61–66.
[24] T. Schiestel, M. Kilgus, S. Peter, K.J. Caspary, H. Wang, J. Caro, Hollow fibre perovskite membranes for oxygen separation, Journal of Membrane Science 258 (2005) 1–4.
[25] S. Liu, G.R. Gavalas, Oxygen selective ceramic hollow fibre membranes, Journal of Membrane Science 246 (2005) 103–108.
[26] A. Leo, S. Liu, J.C.D. da Costa, The enhancement of oxygen flux on $Ba_{0.5}Sr_{0.5}Co_{0.8}Fe_{0.2}O_{3-a}$ (BSCF) hollow fibers using silver surface modification, Journal of Membrane Science 340 (2009) 148–153.
[27] S. Liu, X. Tan, K. Li, R. Hughes, Preparation and characterisation of $SrCe_{0.95}Yb_{0.05}O_{2.975}$ hollow fibre membranes, Journal of Membrane Science 193 (2001) 249–260.
[28] X. Tan, J. Song, X. Meng, B. Meng, Preparation and characterization of $BaCe_{0.95}Tb_{0.05}O_{3-\alpha}$ hollow fibre membranes for hydrogen permeation, Journal of the European Ceramic Society 32 (2012) 2351–2357.
[29] S. Yamanaka, K. Kurosaki, T. Maekawa, T. Matsuda, S. Kobayashi, M. Uno, Thermochemical and thermophysical properties of alkaline-earth perovskites, Journal of Nuclear Materials 344 (2005) 61–66.
[30] R. Ran, Y. Guo, D. Gao, S. Liu, Z. Shao, Effect of foreign oxides on the phase structure, sintering and transport properties of $Ba_{0.5}Sr_{0.5}Co_{0.8}Fe_{0.2}O_{3-\delta}$ as ceramic membranes for oxygen separation, Separation and Purification Technology 81 (2011) 384–391.
[31] X. Meng, N. Yang, J. Song, X. Tan, Z. Ma, K. Li, Synthesis and characterization of terbium doped barium cerates as a proton conducting SOFC electrolyte, International Journal of Hydrogen Energy 36 (2011) 13067–13072.
[32] X. Tan, Y. Liu, K. Li, Mixed conducting ceramic hollow fiber membranes for air separation, AIChE Journal 51 (2005) 1991–2000.
[33] B. Meng, Z. Wang, X. Tan, S. Liu, $SrCo_{0.9}Sc_{0.1}O_{3-\delta}$ hollow fibre membranes for oxygen separation at intermediate temperatures, Journal of the European Ceramic Society 29 (2009) 2815–2822.
[34] J. Guan, S.E Dorris, U. Balachandran, M. Liu, Transport properties of $BaCe_{0.95}Y_{0.05}O_{3-a}$ mixed conductor for hydrogen separation, Solid State Ionics 100 (1997) 45–52.
[35] J.P. Guha, D. Kolar, Phase Equilibria in the system BaO–CeO_2, Journal of Materials Science 6 (1971) 1174–1177.